Mechanistic Studies of Cyclohexanone Monooxygenase: Chemical Properties of Intermediates Involved in Catalysis†

Dawei Sheng, David P. Ballou,* and Vincent Massey*

Department of Biological Chemistry, University of Michigan, Ann Arbor, Michigan 48109-0606

Received June 4, 2001; Revised Manuscript Received July 16, 2001

ABSTRACT: Cyclohexanone monooxygenase (CHMO), a bacterial flavoenzyme, carries out an oxygen insertion reaction on cyclohexanone to form a seven-membered cyclic product, ϵ-caprolactone. The reaction catalyzed involves the four-electron reduction of O_2 at the expense of a two-electron oxidation of NADPH and a two-electron oxidation of cyclohexanone to form ϵ-caprolactone. Previous studies suggested the participation of either a flavin C4a-hydroperoxide or a flavin C4a-peroxide intermediate during the enzymatic catalysis [Ryerson, C. C., Ballou, D. P., and Walsh, C. (1982) *Biochemistry 21*, 2644−2655]. However, there was no kinetic or spectral evidence to distinguish between these two possibilities. In the present work we used double-mixing stopped-flow techniques to show that the C4a-flavin−oxygen adduct, which is formed rapidly from the reaction of oxygen with reduced enzyme in the presence of NADP, can exist in two states. When the reaction is carried out at pH 7.2, the first intermediate is a flavin C4a-peroxide with maximum absorbance at 366 nm; this intermediate becomes protonated at about 3 s^{-1} to form what is believed to be the flavin C4a-hydroperoxide with maximum absorbance at 383 nm. These two intermediates can be interconverted by altering the pH, with a pK_a of 8.4. Thus, at pH 9.0 the flavin C4a-peroxide persists mainly in the deprotonated form. Further kinetic studies also demonstrated that only the flavin C4a-peroxide intermediate could oxygenate the substrate, cyclohexanone. The requirement in catalysis of the deprotonated flavin C4a-peroxide, a nucleophile, is consistent with a Baeyer−Villiger rearrangement mechanism for the enzymatic oxygenation of cyclohexanone. In the course of these studies, the K_d for cyclohexanone to the C(4a)-peroxyflavin form of CHMO was determined to be ~1 μM. The rate-determining step in catalysis was shown to be the release of NADP from the oxidized enzyme.

Cyclohexanone monooxygenase (CHMO)[1] (EC 1.14.13.22), first purified by Trudgill and colleagues from *Nocardia globerula* CL1 (*1*, *2*) and *Acinetobacter* sp. NCIMB 9871 (*1*), is a flavoprotein that catalyzes the reaction shown in eq 1. In this reaction a cyclic ketone is converted to a lactone,

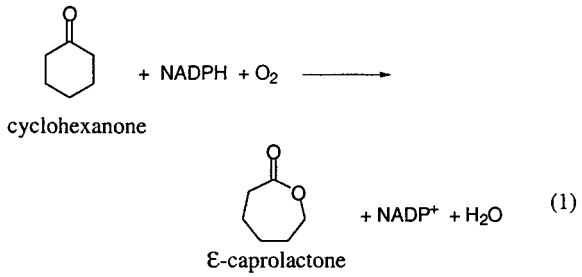

(1)

which can subsequently be hydrolyzed to an aliphatic acid. Under physiological conditions, CHMO catalyzes a key step in the biodegradation of cyclohexanol. Besides its physiological substrate, CHMO can also oxygenate a variety of cyclic ketones (four- to eight-membered rings), aromatic aldehydes, and heteroatom-containing compounds (*3*−*5*). Due to its broad substrate tolerance and its high enantioselectivity, the possibility of using CHMO in synthetic chemistry to produce chiral synthons has aroused much interest (*5*−*7*).

Mechanistically, it has been proposed that a flavin−oxygen adduct, formed from the reaction between the reduced enzyme with oxygen, is the active species during enzymatic catalysis (*8*). From its spectral properties, this flavin−oxygen adduct could be either an enzyme-associated flavin C4a-peroxide ($EFADHOO^-$) or an enzyme-associated flavin C4a-hydroperoxide (EFADHOOH). Here, by spectral rapid kinetic studies of intermediates and of the dependence of their spectra on pH, we provide evidence that the $EFADHOO^-$ is the active oxygenating agent toward the physiological substrate, cyclohexanone. The involvement of the nucleophilic peroxide in the reaction is also consistent with the mechanism proceeding by a Baeyer−Villiger rearrangement. A Baeyer−Villiger rearrangement is defined as an oxygen insertion reaction resulting from the treatment of a ketone with either a peracid or another peroxy compound (*9*). In addition, we have shown that the rate-determining step in catalysis is the release of NADP from oxidized enzyme. We have also shown that cyclohexanone and NADP bind very tightly to the form of CHMO containing the flavin peroxide.

† Financial support was received from the U.S. Public Health Service (GM 20877 to D.P.B. and GM 11106 to V.M.)

* To whom correspondence should be addressed. D.P.B.: e-mail, dballou@umich.edu; phone, 734-764-9582; fax, 734-763-4581. V.M.: e-mail, massey@umich.edu; phone, 734-764-7196; fax, 734-763-4581.

[1] Abbreviations: CHMO, cyclohexanone monooxygenase from *Acinetobacter* sp. NCIMB 9871; EFAD, oxidized form of CHMO; $EFADH_2$, fully reduced form of CHMO; $EFADHOO^-$, flavin C4a-peroxide of cyclohexanone monooxygenase; EFADHOOH, flavin C4a-hydroperoxide of cyclohexanone monooxygenase; FMO, flavin monooxygenase; IPTG, isopropyl β-D-thiogalactopyranoside; KP_i, potassium phosphate buffer; DMF, dimethylformamide.

10.1021/bi011153h CCC: $20.00
Published on Web 08/22/2001

EXPERIMENTAL PROCEDURES

Materials. Cyclohexanone, cyclohexanol, ϵ-caprolactone, NADP (sodium salt), and NADPH were from Sigma-Aldrich. Restriction enzymes *Sal*I and *Nde*I were from Boehringer Mannheim. The polymerase used in the PCR and the kits for the purification of PCR products were obtained from Qiagen.

Culture Medium and Growth of Bacteria. Stock cultures of *Acinetobacter* sp. (NCIMB 9871), obtained from NCIMB Ltd. (Aberdeen, Scotland), were grown on nutrient agar at 30 °C and stored at 4 °C. As reported previously (*1*), cells were grown in media containing the following (g/L): KH_2PO_4, 2.0; Na_2HPO_4, 4.0; $(NH_4)_2SO_4$, 3.0; and yeast extract, 0.2. This solution was adjusted to pH 7.5 and sterilized by autoclaving. At the time of inoculation, concentrated solutions of each of the following compounds were sterilized by membrane filtration and then added to the autoclaved medium to give the indicated final concentration (g/L): $MgSO_4 \cdot 7H_2O$, 0.5; $CaCl_2 \cdot H_2O$, 0.1; $FeSO_4 \cdot 7H_2O$, 0.01; and cyclohexanol, 0.1. This culture medium (100 mL) was inoculated and incubated at 30 °C, with shaking at 150 rpm. After 12 h incubation, additional cyclohexanol was added to a final concentration of 1 g/L, and the culture was incubated for 10 h under the same conditions. The cells were harvested by centrifugation.

Cloning and Expression of CHMO. Genomic DNA was extracted from *Acinetobacter* sp. cells according to the protocol provided by Qiagen. The coding region of CHMO was amplified by PCR with the *Acinetobacter* genomic DNA as the template. The primers used in the PCR were synthesized on the basis of the published DNA sequence (*10*). The 5′ → 3′ sense primer, CGTAATGGAGATTCATATGTCACAAAA, was modified from the genomic DNA to generate both an *Nde*I site (underlined) and an in-frame ATG for initiation. The 5′ → 3′ antisense primer, GACATCCCTGGCAGTCGACTGATGTTAA, was modified from the genomic DNA to generate a *Sal*I site (underlined). The CHMO coding region was amplified, and the PCR product was treated with *Nde*I and *Sal*I. This enzyme-treated PCR fragment was further purified by agarose gel electrophoresis and inserted into a pET-24b vector (Novagen), which was also pretreated with *Nde*I and *Sal*I. The ligation product was transformed into an *E*scherichia *coli* strain, HMS 174 (Novagen). Clones containing the CHMO coding region were isolated from an LB/kanamycin plate. The DNA Sequencing Core Facility at the University of Michigan confirmed the whole sequence of CHMO cDNA.

Growth of Bacterial Cells for Enzyme Expression. An *E. coli* strain of BL21 (DE3) was used for protein expression. LB/kanamycin medium (2 mL) was inoculated with a single colony containing the DNA coding region for CHMO. This was grown for 12 h at 37 °C with shaking at 250 rpm. This medium was used to inoculate 150 mL of LB/kanamycin medium, which was incubated at 22 °C for 12 h with shaking at 250 rpm. Ten milliliters of this medium was used to inoculate 1000 mL of LB/kanamycin medium. After 6 h of incubation at 22 °C with shaking at 250 rpm, IPTG was added to a final concentration of 10 μM, and the cells were harvested after an additional 18−22 h incubation at 22 °C with shaking at 250 rpm.

Enzyme Purification. All enzyme purification steps were performed at 4 °C. Cells were harvested by centrifugation at 8000*g* for 20 min, washed once by suspension in 50 mM Tris and 2 mM EDTA buffer (pH 8.0), centrifuged again, and finally suspended in 20 mM KP_i, pH 7.2. The cells were disrupted by ultrasonication, and cell debris was removed by centrifugation at 25000*g* for 30 min. The supernatant was treated with $(NH_4)_2SO_4$, and the fraction that precipitated between 50% and 90% saturation was retained. It was dissolved in 20 mM KP_i (pH 7.2) and dialyzed overnight against 6 L of the same buffer.

Ion-Exchange Chromatography. The dialyzed fraction was loaded onto a DEAE-Sepharose column that was preequilibrated with KP_i (20 mM) and EDTA (2 mM), pH 7.2. Elution was developed with a linear gradient formed by mixing 500 mL of 0.5 M KCl in the above buffer into 500 mL of the same buffer without KCl. The fractions were analyzed by absorbance at 280 and 440 nm, as well as by the enzyme activity toward cyclohexanone. Fractions containing activity were pooled and subjected to $(NH_4)_2SO_4$ precipitation (90%) and then dialysis.

Red A Matrix Affinity Chromatography. The published protocol (*10*) was slightly modified. The CHMO protein from ion-exchange chromatography was applied to a column containing 150 mL of Amicon Red A matrix agarose (Amicon), which was preequilibrated with KP_i (20 mM) and FAD (10 μM) at pH 7.2. The fraction (150 mg of protein) containing CHMO was loaded, and the column was washed with 300 mL of the preequilibrating buffer. Then 5 mM ATP and 400 mM KCl in the same buffer were applied to elute the enzyme. Fractions containing enzyme with activity toward oxygenating cyclohexanone were pooled. The excess ATP, KCl, and FAD were removed by dialysis. SDS−PAGE analysis showed that the CHMO from this purification procedure was essentially homogeneous. The specific activity of the enzyme is 23 units/mg (1 unit is defined by 1 μmol of NADPH oxidation in 1 min at pH 9.0 and 25 °C).

Steady-State Enzymatic Assay. CHMO activity was routinely assayed at 25 °C by monitoring NADPH oxidation at 340 nm with a Cary 219 spectrophotometer. A typical assay solution contained 1 mL of air-equilibrated 0.1 M glycine/NaOH, pH 9.0, 160 μM NADPH, and 0.016 μM CHMO. The reaction was initiated by the addition of 50 μM cyclohexanone. For correlation with stopped-flow half-reaction data, steady-state turnover was also measured at 4 °C in the presence of 0.4 M KCl. For these measurements, NADPH oxidation at 340 nm was monitored with a Hi-Tech stopped-flow instrument. Enzyme, final concentration after mixing of 1−3 μM in 0.1 M glycine/NaOH plus 0.4 M KCl, was supplemented with 13 μM FAD to maintain full enzyme activity and was mixed with air-saturated solutions of the same buffer containing 10−200 μM cyclohexanone at concentrations of 20−80 μM NADPH. One data set was also collected using O_2-equilibrated solutions of substrates.

Rapid Reaction Studies. Both the reduction of the enzyme by NADPH and the reoxidation of the reduced enzyme in the presence of oxygen and substrates were investigated by stopped-flow spectrophotometric techniques at 4 °C. The reductive half-reactions were carried out under anaerobic conditions with a Kinetic Instruments stopped-flow spectrophotometer. The reaction mixtures contained equal volumes of the following two solutions: (1) approximately 9

μM CHMO in either 0.1 M glycine/NaOH, pH 9.0, or 0.1 M KP_i, pH 7.2; (2) NADPH (18−220 μM) with or without 400 μM cyclohexanone in the same buffers as those in solution 1. The anaerobic reduction of the enzyme-bound flavin chromophore was followed by the decrease in absorbance at 440 nm. The observed rate constants were obtained using Program A (developed by Chun-Jen Chiu, Rong Chang, Joel Dinverno, and Dr. David P. Ballou, University of Michigan) by fitting the plot of absorbance at 440 nm vs time. The oxidative half-reactions were carried out using a Hi-Tech Scientific SF-61 single-mixing or a Hi-Tech Scientific DX-2 stopped-flow spectrophotometer with sequential mixing. The instruments were used with either diode array or single wavelength detection. CHMO was reduced photochemically as previously described (*11*). Typically, in sequential mixing experiments, the enzyme solution consisted of ~100 μM CHMO in 5 mM KP_i, 0.4 M KCl,[2] 20 mM EDTA, and 1.5 μM deazaflavin at pH 7.2. After the enzyme was photoreduced anaerobically, neutralized NADP from the sidearm of the tonometer was introduced into the enzyme solution to a final concentration of 150 μM. In the stopped-flow spectrophotometer, the enzyme solution was first mixed with air-saturated buffer (5 mM KP_i, 0.4 M KCl, pH 7.2). After times ranging from 0.02 to 1.5 s, this solution was mixed with an equal volume of more concentrated buffer at the indicated pH that contained substrate as described in the figure legend. After the second mixing, either multiwavelength diode array or single wavelength photomultiplier detection was employed to monitor the reaction mixture, which was maintained at 4 °C. For single-mixing experiments, reduced enzyme was prepared as above, but at approximately half the concentration, and was reacted with air-saturated buffer containing cyclohexanone. Details of individual stopped-flow experiments are described in the figure legends and the text.

Determination of the Redox Potential. The redox potential of CHMO was determined by the method of Massey (*12*). Enzyme (20 μM) in the presence of 0.1 M KP_i, pH 7.0, 2 μM benzyl viologen, 42 μM anthraquinone-2-sulfonate, and 140 μM xanthine was made anaerobic in a cuvette with a sidearm by repeated cycles of evacuation and equilibration with O_2-free argon. After equilibration at 25 °C, reduction was initiated by mixing in 30 nM xanthine oxidase, and spectra were recorded at appropriate intervals until reduction of both dye and enzyme was complete (~2 h). Reduction of the dye was measured at 340 nm, the isosbestic point for reduction of enzyme, and reduction of the enzyme was monitored at 354 nm, an isosbestic point for reduction of the dye (E_m = −225 mV).

RESULTS

Enzyme Expression and Purification. CHMO was expressed and purified as described in Experimental Procedures. The CHMO coding region was inserted into a pET-24b vector containing a T7 promoter, transformed into *E. coli* BL21 (DE3) cells, and expressed at a relatively low temperature (22 °C) and a low concentration of IPTG (10 μM). These conditions were required to obtain good yields of soluble protein. Homogeneous CHMO (≥95% as estimated by SDS−PAGE) was obtained after ammonium sulfate fractionation and two chromatographic steps. The yield of homogeneous CHMO was 60−80 mg/L of culture medium, which is considerably higher than that of the expression system (8−9 mg/L) previously reported (*10*). The spectral and general kinetic parameters (k_{cat} and K_m for cyclohexanone and for NADPH) of the enzyme purified from our expression system are essentially identical to those of the enzyme purified from *Acinetobacter* sp. (*1*).

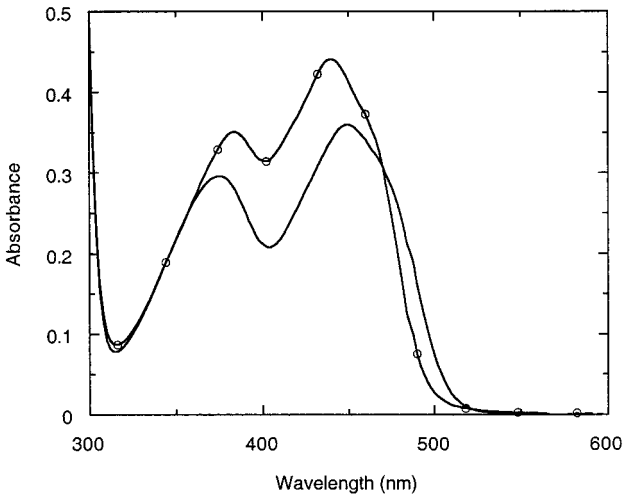

FIGURE 1: Determination of the molar absorbance of the flavin in CHMO. Enzyme in 0.05 M NaP_i, pH 7.2, 25 °C, was denatured by adding sodium dodecyl sulfate (to 0.1%), and the spectra were recorded until no further changes were observed (10 min). Centrifuging the solution through a Centricon 30 membrane verified that all of the FAD was in the filtrate; thus, the FAD was completely released from the protein by the SDS treatment. The final spectrum of the enzyme had no absorbance in the visible region. Spectrum of CHMO before adding SDS (−○−). Spectrum of CHMO after adding SDS and waiting 10 min (—).

Determination of the Extinction Coefficient. Cyclohexanone monooxygenase has a somewhat unusual spectrum for a flavoprotein; it has rather highly absorbing maxima at 384 and 440 nm with less than usual resolution between the two peaks. The extinction coefficient of CHMO was determined from the concentration of free FAD released from the enzyme after addition of 0.1% sodium dodecyl sulfate (Figure 1). The free FAD concentration was determined from its extinction of 11 300 M^{-1} cm^{-1} at 450 nm (*13*). From this, the extinction coefficient of CHMO before addition of sodium dodecyl sulfate was determined to be 13 800 M^{-1} cm^{-1} at 440 nm.

Determination of the Redox Potential. The redox potential of the enzyme was found to be very close to that of anthraquinone-2-sulfonate. Both the enzyme and the anthraquinone-2-sulfonate were reduced in nearly equivalent proportions throughout the experiment when reduction was initiated by addition of xanthine oxidase in the presence of xanthine and benzyl viologen as described in Experimental Procedures. From the difference in the log(ox/red) of the enzyme vs log(ox/red) of the dye, it can be estimated that the enzyme has a potential that is 8 ± 1 mV more positive than that of the dye (E_m = −225 mV), i.e., −217 ± 1 mV.

[2] KCl (0.4 M) was included so that in the pH-jump experiments any effects of ionic strength changes would be minimized. The presence of potassium chloride had no significant effect on the rate constants or on the oxygenation stoichiometry, which was ≥95% coupled to NADPH utilization.

Table 1: Kinetic Parameters for Reduction of CHMO by NADPH[a]

pH	K_d (μM)	k_{red} (s^{-1})	k_{red}/K_d ($M^{-1}\,s^{-1}$)
9.0	6.8	22	3.2×10^6
7.2	7.0	24	3.4×10^6
9.0	7.9	20	2.5×10^6
7.2[b]	7.5	21	2.8×10^6

[a] All experiments were carried out at 4 °C. For details see Experimental Procedures. [b] The reaction was carried out in the presence of 200 μM cyclohexanone. Estimates for uncertainties are ± 1 μM for K_d values and ± 2 s^{-1} for k_{red} values.

Steady-State Kinetics. The kinetics of catalytic turnover were measured in the presence of 0.4 M KCl at pH 9.0, 4 °C, to correlate with pre-steady-state kinetic data determined in stopped-flow experiments. There was very little effect on changing the cyclohexanone concentration in the range 5−100 μM and no detectable effect caused by changing the oxygen concentration between 120 and 740 μM. There was a slight increase in velocity with increasing NADPH concentration, permitting the determination of k_{cat} at 1.3 s^{-1} and $K_{m,NADPH}$ as ~10 μM. The K_m values for cyclohexanone and oxygen could not be determined accurately, but from the lack of response in the concentration ranges used, they can be estimated to be <1 μM and ≤10 μM, respectively.

Rapid Reaction Kinetics. In stopped-flow spectrophotometric experiments, we were able to detect and identify several intermediates in the reaction and also to determine the rate constants of specific catalytic steps. The chemical reactions catalyzed by CHMO can be studied in terms of two half-reactions; in the reductive half-reaction, enzyme-bound FAD is reduced by NADPH, and in the oxidative half-reaction, reduced enzyme-bound FAD is reoxidized by oxygen alone, by oxygen in the presence of NADP, or by oxygen in the presence of both NADP and the substrate cyclohexanone. To investigate each partial reaction separately, the enzyme was kept under anaerobic conditions before being mixed with reactants in the stopped-flow spectrophotometer.

Reductive Half-Reaction. Pseudo-first-order rate constants for the reduction of enzyme-bound flavin by NADPH were determined at 4 °C under anaerobic conditions at pH 9.0 and at pH 7.2 by monitoring the decrease in absorbance at 440 nm that was due to the enzyme-bound oxidized flavin. The kinetic traces could be fit to single-exponential equations to determine the k_{obs} values. Plots of k_{obs} vs NADPH concentrations approach limiting values and can be described by eq 2a, consistent with an equilibrium reaction that precedes the hydride transfer from NADPH to oxidized flavin as shown in eq 2b. The dissociation constant ($K_{d,NADPH}$) and

$$k_{obs} = k_{red}[\text{NADPH}]/(K_{d,NADPH} + [\text{NADPH}]) \quad (2a)$$

$$\text{EFAD} + \text{NADPH} \overset{K_{d,NADPH}}{\rightleftharpoons} \text{EFAD}\cdot\text{NADPH} \xrightarrow{k_{red}} \text{EFADH}^-\cdot\text{NADP}^+ \quad (2b)$$

the first-order rate constant (k_{red}) were determined from eq 2a (*14*). Values for $K_{d,NADPH}$ and for k_{red} for CHMO are summarized in Table 1. The presence of the substrate, cyclohexanone, has no effect on the values of $K_{d,NADPH}$ or k_{red}. However, in aerobic steady-state assays, cyclohexanone increases the rate of NADPH consumption by >50-fold. This implies that the presence of substrate only affects reactions involving oxygen.

Oxidative Half-Reaction. The oxidative half-reactions were studied with CHMO that had been previously reduced anaerobically either by photochemical methods in the presence of 5-deazaflavin and EDTA (*11*) or by a system using xanthine oxidase and xanthine in the presence of the electron-transfer mediator, benzyl viologen (*12*). The reduced enzyme was reoxidized at 4 °C by three different protocols: (a) reduced enzyme was mixed with oxygenated buffer alone (eq 3a), (b) reduced enzyme in the presence of NADP was mixed with oxygenated buffer (eq 3b), or (c) reduced enzyme in the presence of NADP was mixed with oxygenated buffer containing cyclohexanone (eq 3c).

Reaction of the Reduced Enzyme with Oxygen. When the reduced enzyme was mixed with oxygen alone, the spectrum observed in the dead time of the stopped-flow apparatus was that of the reduced enzyme, and this converted in a single phase to the oxidized form. No intermediates of any sort were detected during the oxidation of reduced enzyme by oxygen. A plot of the observed rate constant of this reaction vs oxygen concentration is linear and yields a second-order rate constant of 1.7×10^3 M^{-1} s^{-1} at pH 9.0, 4 °C, in the presence of 0.4 M KCl.

$$\text{E FADH}_2 + \text{O}_2 \xrightarrow{k_{ox}} \text{E FAD} + \text{H}_2\text{O}_2 \quad (3a)$$

$$\text{NADP}^+\cdot\text{EFADH}_2 + \text{O}_2 \xrightarrow{> 5 \times 10^6\ M^{-1}s^{-1}} \text{NADP}^+\cdot\text{EFADHOO}^- \underset{pK_a = 8.4}{\overset{H^+}{\rightleftharpoons}} \text{NADP}^+\cdot\text{EFADHOOH}$$

$$\downarrow$$

$$\text{EFAD} + \text{NADP}^+ + \text{H}_2\text{O}_2 \quad (3b)$$

$$\text{NADP}^+\cdot\text{EFADH}^- + \text{O}_2 \longrightarrow \text{NADP}^+\cdot\text{EFADHOO}^- \xrightarrow{\text{cyclohexanone}} \text{EFAD} + \varepsilon\text{-caprolactone} + \text{NADP}^+ + \text{H}_2\text{O} \quad (3c)$$

Reaction of the Reduced Enzyme with Oxygen in the Presence of NADP. At 4 °C, pH 7.2, in the presence of NADP (~1.5 equiv/equiv of enzyme), the reduced enzyme reacted very rapidly with oxygen to form an intermediate with a λ_{max} of 366 nm. The spectrum of the intermediate is shown in Figure 2A. Because this reaction was complete in the dead time of the stopped-flow apparatus (~2 ms), even when only stoichiometric concentrations of oxygen were used, kinetic traces are not shown. However, these results lead us to conclude that the second-order rate constant for reaction with oxygen is $\geq 5 \times 10^6$ M^{-1} s^{-1}, which is at least 3000-fold greater than that in the absence of NADP (see above). As shown in Figure 2A, at pH 7.2, the intermediate with a λ_{max} of 366 nm converted into a second species with a λ_{max} of 383 nm within 1.5 s ($k = 3.3$ s^{-1}). At wavelengths greater than 450 nm, absorbance of neither intermediate shows any significant increases over that of reduced enzyme; thus, in the 1.5 s of observation, Figure 2 shows that essentially no oxidized enzyme was formed during this conversion. The intermediates are likely to be the flavin C4a-peroxide and C4a-hydroperoxide forms of the enzyme (see Discussion).

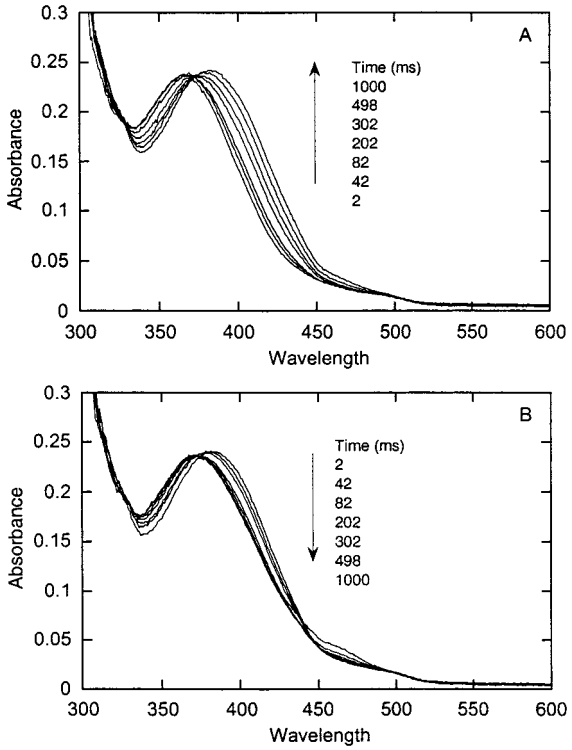

FIGURE 2: Spectra of the postulated EFADHOO$^-$and EFADHOOH species formed between reduced CHMO and oxygen in the presence of NADP. The spectra were recorded with a double-mixing stopped-flow spectrophotometer at 4 °C. (A) Reduced CHMO (98 μM), NADP (500 μM), KP_i (5 mM), and KCl (0.4 M), pH 7.2, were mixed with air-saturated KP_i (5 mM) and KCl (0.4 M), pH 7.2. After 10 ms, this was diluted with an equal volume of air-saturated KP_i (5 mM) and KCl (0.4 M), pH 7.2. (B) Same as (A) except that the first two solutions were incubated for 1.5 s (to form the putative hydroperoxyflavin). Air-saturated glycine (100 mM) and KCl (0.4 M), pH 9.0, were then added in the second mixing. The final pH was 8.8. All spectra were recorded at the indicated times after the second mixing.

A series of pH-jump experiments were carried out to discern whether these two intermediates were consistent with being the flavin C4a-peroxide and flavin C4a-hydroperoxide forms of the enzyme. The stopped-flow apparatus in the double-mixing mode was used to first mix reduced enzyme with oxygen at one pH in dilute buffer. This was aged for a defined period of time and then mixed with a higher concentration of a second buffer to quickly change the pH. In a typical experiment, as shown in Figure 2B, the reduced enzyme in the presence of NADP was mixed with air-saturated 5 mM phosphate containing 0.4 M KCl at pH 7.2 and incubated for 1.5 s to permit the formation of the intermediate with a λ_{max} of 383 nm. Then, air-saturated 100 mM glycine at pH 9.0 also containing 0.4 M KCl was added in the second mixing step to give a final pH of 8.8. The species with a λ_{max} of 383 nm converted at 4.7 s^{-1} back to the species with a λ_{max} of 366 nm. During this conversion, there was only a small amount of absorbance generated at 450 nm, indicating the formation of about 5−10% of oxidized enzyme. Similar experiments were carried out using several buffers that give a series of different final pH values. Equation 3b describes the equilibrium presumed to be established in the experiment. The logarithm of the ratio of concentrations of the 366 nm species to the 383 nm species that developed by 1.5 s after adjustment to the new pH is plotted vs pH in Figure 3. Using eq 4, a pK_a of 8.4 ± 0.2 for this conversion can be calculated.

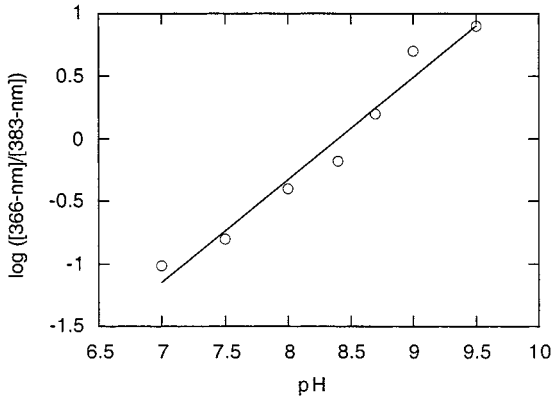

FIGURE 3: Plot of log([366 nm species]/[383 nm species]) vs pH. Photoreduced CHMO (38 μM) in the presence of NADP (57 μM) in the indicated pH buffer was mixed with air-saturated buffer with the same pH. After 2 s of the reaction, the ratio between 366 nm species and 383 nm species was calculated. For calculating the ratio, it was assumed that, at pH 7, all of the intermediate is the 383 nm species and, at pH 9.5, all of the intermediate is the 366 nm species (see Figure 2). KP_i buffer (20 mM), pH 7.0 and 7.5, TAPS (20 mM), pH 8.0 to 8.7, and glycine, pH 9.0 to 9.5, were used in the reaction. All experiments were carried at 4 °C in the presence of 0.4 M KCl.

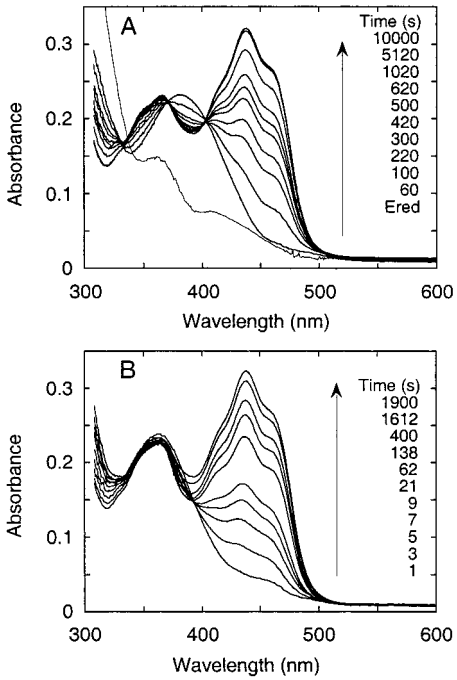

FIGURE 4: Spectra of the reaction between photoreduced CHMO and oxygen in the presence of NADP at pH 7.2 and at pH 9.0. Photoreduced CHMO (38 μM) in the presence of NADP (57 μM) was mixed with air-saturated buffer. The reaction was carried out at 4 °C. The spectra were recorded at the indicated times. (A) Spectra of the reaction at pH 7.2 in KP_i (20 mM) and KCl (0.4 M). (B) Spectra of the reaction at pH 9.0 in 0.1 M glycine/NaOH and 0.4 M KCl.

$$pK_a = pH - \log\left(\frac{[366\ \text{species}]}{[383\ \text{species}]}\right) \quad (4)$$

The proposed flavin C4a-hydroperoxide is very stable at 4 °C, pH 7.2, when no substrate is present. In Figure 4A, the spectrum recorded after 60 s of reaction between oxygen

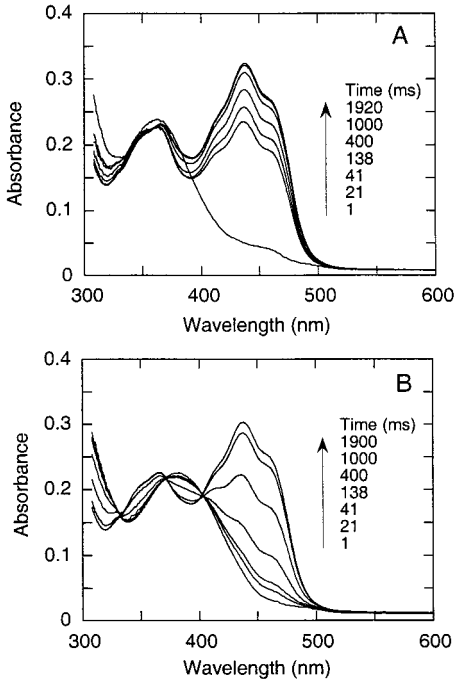

FIGURE 5: Spectra of the reactions between cyclohexanone and EFADHOO$^-$ and EFADHOOH at 4 °C. The spectra were recorded with a double-mixing stopped-flow spectrophotometer equipped with a diode array. (A) Reduced CHMO (95 μM), NADP (500 mM), KP_i (5 mM), and 0.4 M KCl, pH 7.2, were mixed with air-saturated KP_i (5 mM) and 0.4 M KCl, pH 7.2. After 15 ms incubation, a third solution containing cyclohexanone (200 mM) in glycine (100 mM) and KCl (0.4 M), pH 9.0, was introduced into the previously mixed solution. (B) The same as (A) except that the third solution was added after 1.5 s incubation of the first two solutions. All spectra were recorded at the indicated times after the second mixing.

and reduced CHMO in the presence of NADP showed a maximum absorbance of 383 nm, almost identical with that observed in Figure 2A at 1 s. This species slowly converted to oxidized enzyme within 60 min with isosbestic points at 370 and 405 nm, suggesting that no significant buildup of intermediates occurred during the conversion of flavin C4a-hydroperoxide to oxidized enzyme. The proposed flavin C4a-peroxide is somewhat less stable, as shown in Figure 4B, where the reduced enzyme in the presence of NADP was reacted with O_2 at 4 °C, pH 9.4. Under these conditions the half-life of the intermediate was ca. 12 s, about 25-fold shorter than that for the intermediate at pH 7.2.

Reaction of the Reduced Enzyme with Oxygen in the Presence of NADP and Cyclohexanone. Experiments were also carried out in the double-mixing mode as above, except that cyclohexanone was included in the second mix. Mixing oxygen with the reduced enzyme in complex with NADP at pH 7.2 formed the 366 nm species very rapidly, as described in the previous section. When cyclohexanone in 0.1 M glycine, pH 9.0, was mixed with this species within 20 ms, oxidized enzyme was quickly formed. Approximately 70% of the reaction was complete within 21 ms after the second mix (Figure 5A). The remainder of the oxidized enzyme formed according to more complicated kinetics (see below). In contrast, when the 366 nm species was incubated at pH 7.2 for 1.5 s, which fully formed the 383 nm species (Figure 5B), and then was mixed with pH 9.0 buffer containing cyclohexanone, oxidized enzyme was formed much more slowly.

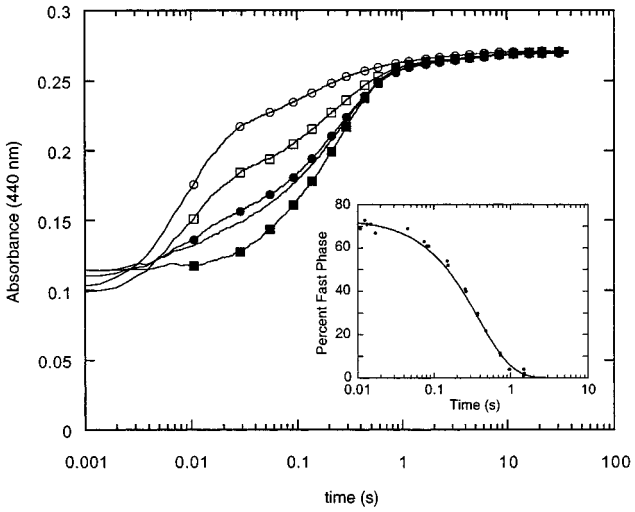

FIGURE 6: Kinetics of reaction of the CHMO oxygenated intermediate reacting with cyclohexanone as a function of incubation time at pH 7.2. Conditions were the same as in Figure 5 except the enzyme concentration was ~80 μM in the first syringe. The reduced enzyme in the presence of NADP was preincubated with oxygen for different periods of time: (○) 12 ms, (□) 45 ms, (●) 86 ms, (—) 260 ms, and (■) 1500 ms. After the indicated time of premixing, an equal volume of solution containing cyclohexanone (200 μM) in pH 9.0 buffer was introduced, and the reactions were followed at 440 nm. Inset: Percent of the reaction occurring in the fast phase as a function of aging time at pH 7.2 before being mixed with cyclohexanone at pH 9.0. The smooth line is a fit with a k_{obs} = 2.65 s^{-1}.

A series of experiments were carried out by reacting reduced enzyme at pH 7.2 in the presence of NADP with oxygen in the first mix and then, after various times, introducing cyclohexanone in the second mix at pH 9.0. The reactions were followed at 440 nm (Figure 6). The rate constants for each of the phases did not change, but the extents of reaction occurring in the two fastest phases were dependent on the time that elapsed between the primary mix of O_2 with the reduced enzyme and NADP, and before the secondary mix with cyclohexanone. The amplitude of the fast phase (k = 110 ± 5 s^{-1}) decreases with increasing preincubation time, and this is compensated by a corresponding increase in amplitude of the second phase (k = 5 ± 1 s^{-1}). The final phase (k = 0.3 ± 0.1 s^{-1}) accounts for about 4% the total absorbance change and is independent of the preincubation time. Representative traces are shown in Figure 6. The inset of this figure shows a plot of the percentage of the reaction in the fast phase as a function of the preincubation time. From this plot a rate constant of 2.7 ± 0.1 s^{-1} can be calculated for the conversion to the nonreactive species. These observations are consistent with the fast phase being due to the oxygenated flavin intermediate that absorbs at 366 nm reacting with cyclohexanone to form product and the slow phase being due to that fraction of enzyme that has converted to the nonreactive 383 nm species during the incubation that now converts back to the reactive species at ~5 s^{-1} before reacting with substrate. The reaction was also followed in the single-mixing mode of the stopped-flow instrument so that there was no preincubation period. In this experiment reduced enzyme at pH 9, 4 °C, in the presence of 0.4 M KCl and 1.5 equiv of NADP was mixed with air-saturated excess cyclohexanone in the same buffer, and the reaction was followed at 5−10 nm intervals in the visible

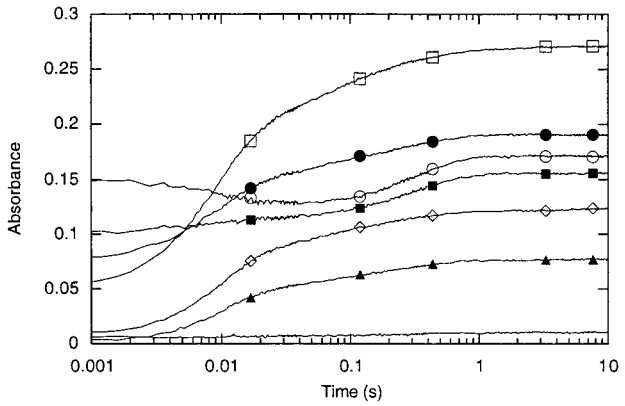

FIGURE 7: Reaction traces at selected wavelengths for the reaction of photoreduced CHMO with air-equilibrated cyclohexanone. CHMO (21.3 μM) containing NADP (32.4 μM) was reacted with cyclohexanone (49 μM) in the stopped-flow spectrophotometer (concentrations after mixing). Each reactant was in glycine/NaOH (0.1 M), pH 9.0, containing KCl (0.4 M), 4 °C. Wavelengths used are (—) 500 nm, (◇) 475 nm, (■) 395 nm, (○) 380 nm, (●) 410 nm, and (□) 440 nm.

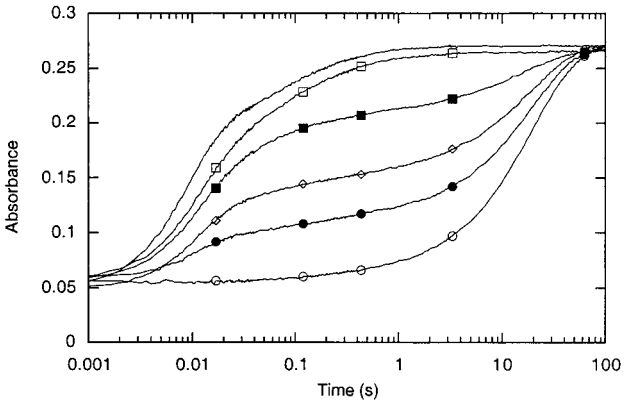

FIGURE 8: Traces at 440 nm for the reaction of CHMO with air-equilibrated buffer and varying concentrations of cyclohexanone. Conditions were the same as in Figure 7 except that the concentration of cyclohexanone was varied. Cyclohexanone concentrations: (○) 0, (●) 5.3 μM, (◇) 10.6 μM, (■) 16 μM, (□) 21 μM, and (—) 48.5 μM (concentrations after mixing).

range of the spectrum. Selected traces are shown in Figure 7. At all wavelengths the data are fit very well with rate constants of 115 ± 5, 12 ± 1, and 3 ± 0.2 s^{-1}. As will be detailed in the Discussion section, we believe these rate constants to be associated respectively with (a) the oxygenation of the substrate and formation of the oxidized enzyme, (b) dissociation of the ϵ-caprolactone product, and, finally, (c) dissociation of NADP.

In the single-mix experiment described in the last paragraph, the solution of reduced enzyme plus 1.5 equiv of NADP was also reacted with air-equilibrated buffer at pH 9.0 without any substrate and with various concentrations of cyclohexanone, many of which were substoichiometric with respect to the enzyme. Results are shown in Figure 8. In the absence of cyclohexanone, the formation of oxidized enzyme is essentially monophasic, with ~92% of the absorbance change associated with a rate constant of 0.05 s^{-1}; the remaining absorbance change is associated with a rate constant of ~3 s^{-1}. With increasing concentrations of cyclohexanone, the reaction traces become multiphasic and are fitted well with the same three rate constants found for the reactions described in Figure 7 (115 ± 5, 12 ± 1, and 3 ± 0.2 s^{-1}). In addition, there was a small change in absorbance occurring at 0.05 s^{-1} as observed in the absence of cyclohexanone. The extent of absorbance change in the fast phase is essentially stoichiometric with substrate concentration until an excess over that of the enzyme is reached, whereupon little further change is observed. These results indicate very tight binding of cyclohexanone to the reactive flavin C4a-peroxide intermediate, with a $K_d \leq 1$ μM.

Binding of NADP to the Reduced Enzyme. From the preceding experiments it is clear that formation of the reactive flavin C4a-peroxide requires that the reduced enzyme be in complex with NADP. There are only minor changes in the absorbance spectrum when NADP is bound to reduced enzyme, making determination of K_d difficult by conventional spectrophotometric titrations. We therefore characterized the extent and the rate of this interaction more fully by making use of the spectral changes associated with the very rapid formation of the C4a-peroxide at 366 nm (Figure 2), which only happens when NADP is bound to the reduced enzyme (see above). These experiments involved use of the stopped-flow instrument in the double-mixing mode, where reduced enzyme at pH 7.2 was mixed with different concentrations of NADP in the primary mix, allowed to age for various times, and then reacted with oxygen in the second mix. It was found that the binding of NADP to reduced enzyme was a comparatively slow and complex process, and the rapid formation of the C4a-peroxide required a preincubation time of >500 ms for optimal yield. For example, an aging time of 20 ms for the reduced enzyme with a 1.5-fold excess of NADP before mixing with oxygen (240 μM) resulted in full formation of the C4a-peroxide in a complex reaction with an overall half-time of ~80 ms. By contrast, an aging time of 100 ms before mixing with oxygen resulted in formation of C4a-peroxide with an overall half-time of ~20 ms. When preincubation times before mixing with oxygen were ≥500 ms, only a single phase was observed with $t_{1/2}$ values of ~2 ms for the formation of the 366 nm absorbing species. Therefore, for study of the dependence of the overall process on NADP concentration, an aging time of 5 s was employed. Under these conditions the amplitude of the absorbance increase was directly proportional to NADP concentration until 1:1 stoichiometry with the enzyme flavin was reached; higher concentrations resulted in no further increase (results not shown). These results indicate very tight binding of NADP to the reduced enzyme, and a K_d of ≤1 μM can be estimated.

Binding of NADP to the Oxidized Enzyme. Titration of oxidized CHMO with NADP results in a considerable decrease in enzyme flavin absorbance in the 390 nm region, with a shift in the absorbance maximum from 383 to 366 nm (Figure 9). Use was made of this spectral change to determine the kinetics and thermodynamic features of the binding of NADP to the enzyme. Oxidized enzyme in 0.1 M glycine/NaOH, pH 9.0, plus 0.4 M KCl was mixed at 4 °C with equal volumes of various concentrations of NADP in the same buffer, and the absorbance changes at 388 and 440 nm were followed in the Hi-Tech SF-61 stopped-flow spectrophotometer. At least four reaction traces were collected at each NADP concentration and averaged for increased signal-to-noise ratios before analysis. Spectra of the completed reaction mixtures were also recorded and

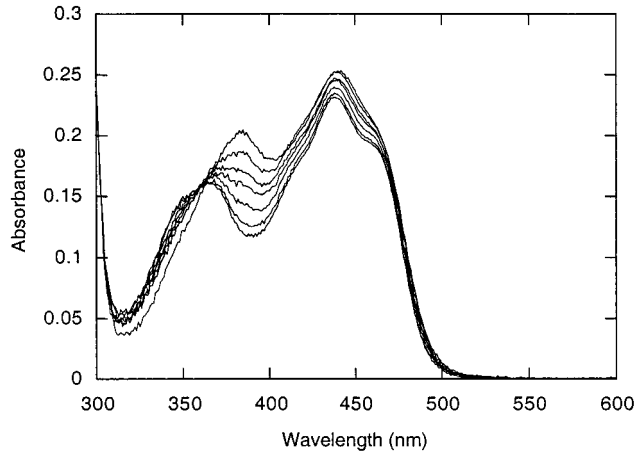

FIGURE 9: Spectra recorded in the stopped-flow spectrophotometer of the reaction mixtures after mixing CHMO (18.8 μM) with various concentrations of NADP at 4 °C in glycine/NaOH (0.1 M) containing KCl (0.4 M), pH 9.0 (all concentrations after mixing). All spectra are also corrected for the tail of absorbance of the NADP extending out to ~360 nm. Sequential spectra from those with the highest absorbance to those with the lowest at 390 nm correspond to 0, 13.75, 27.5, 45.8, 91.5, 162.5, and 379 μM NADP.

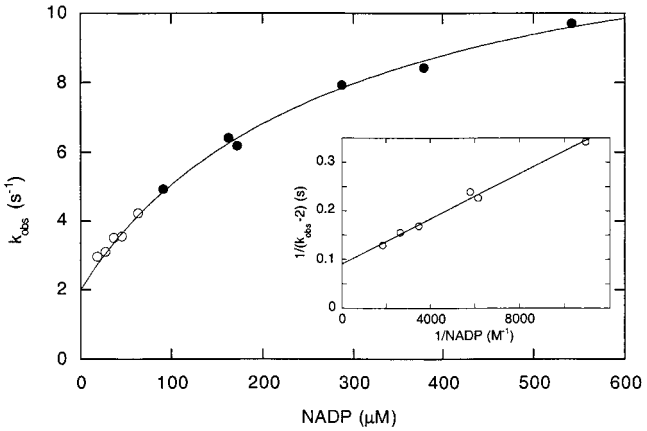

FIGURE 10: Kinetic analysis of the reaction traces obtained in the experiment of Figure 9 (see text for details). Because of the concentration of enzyme used in the experiment, only the primary data given by the solid circles (i.e., ≥100 μM) were used for the fit and in the determination of k_4. However, all of the data are plotted. The primary plot shows k_{obs} vs [NADP]. This gives a *y*-intercept value of 2.0 s^{-1} (k_4 in eq 5). Inset: $1/(k_{obs} - k_4)$ vs 1/[NADP] for the highest concentrations of NADP used. The *y*-intercept of this plot yields $1/k_3$ ($k_3 = 11.5$ s^{-1}), and the slope/intercept yields the ratio $k_2/k_1 = 2.5 \times 10^{-4}$ M. From this analysis, the thermodynamic K_d for the binding of NADP can be calculated from the expression $K_d = k_2k_4/[k_1(k_3 + k_4)] = 37$ μM.

averaged for each concentration of NADP used, as well as that of the NADP alone. Thus, thermodynamic and kinetic properties of the reaction could be compared in the same experiment. At each concentration of NADP, even those that were substoichiometric with the enzyme, more than 90% of the absorbance change could be fit with an observed rate constant that varied with the NADP concentration. A minor phase, comprising a change at 388 nm of only about 0.005 absorbance unit, was too small to permit meaningful analysis but on average had a k_{obs} of ~0.1 s^{-1}. The dependence of k_{obs} for the major change with NADP concentration is shown in Figure 10, with a finite intercept on the *y*-axis, indicative of a two-step binding process (*14*) as indicated in eq 5. A

$$E_{ox} + NADP \underset{k_2}{\overset{k_1}{\rightleftharpoons}} E_{ox}\cdot NADP \underset{k_4}{\overset{k_3}{\rightleftharpoons}} E_{ox}NADP^* \qquad (5)$$

secondary plot of $1/(k_{obs} -$ intercept) vs 1/[NADP] is shown in the inset to Figure 10. The value of k_4 is determined as ~2 s^{-1} from the *y*-intercept of the primary plot. The value for k_3 is determined as 11.5 s^{-1} from the reciprocal of the *y*-axis intercept of the secondary plot, and the ratio k_2/k_1 is determined as 2.55×10^{-4} M from the slope/intercept ratio of the secondary plot (*14*). For a two-step binding equilibrium the thermodynamic $K_d = k_2k_4/[k_1(k_3 + k_4)] = 37$ μM. This is in excellent agreement with the value determined from the overall spectral change recorded in the experiment. For this purpose the ΔA_{388} values at high concentrations of NADP were used in a double-reciprocal plot to estimate the theoretical maximum change that would be associated with full complex formation in the experiment ($\Delta A_{388} = 4840$ M^{-1} cm^{-1}). This ΔA_{388} value was then used to calculate the concentration of free and bound NADP and that of the E_{ox}·NADP* complex at each concentration of NADP used in the experiment. The K_d was calculated from eq 6 at each step of the titration. For all 12 concentrations of NADP used, even those that were substoichiometric with the enzyme, the range of calculated K_d values was 25−38 μM, with the majority close to the average value of 32 μM.

$$K_d = \frac{[E_{ox}\cdot NADP]}{[E_{ox}]_{free}[NADP]_{free}} \qquad (6)$$

It was also noted that as the NADP concentration was increased, a progressively larger loss of absorbance occurred within the dead time (~3 ms) of the stopped-flow instrument. This is consistent with the two-step equilibrium of eq 5, with E_{ox}·NADP formed in rapid equilibrium in the first step. This first intermediate exhibited a spectrum with absorbance that is intermediate between that of free enzyme and that of the final complex in the range 370−420 nm. A double-reciprocal plot of the absorbance missing in the dead time versus the NADP concentration indicates a decrease in ϵ_{388} of 2900 M^{-1} cm^{-1} for formation of the primary complex and a K_d of 2.3 $\times 10^{-4}$ M (data not shown). This is in close agreement with the kinetic analysis of Figure 10 for k_2k_1.

DISCUSSION

CHMO is a bacterial flavoprotein monooxygenase that catalyzes the reaction of cyclohexanone, NADPH, and O_2 to form the cyclic ϵ-caprolactone, NADP, and water as shown in eq 1. The oxygenation of ketones by CHMO is largely limited to cyclic ketones; however, cyclic ketones containing four to eight carbons are all reasonable substrates (*7*, *15*). These reactions catalyzed by CHMO are classified as Baeyer−Villiger reactions. However, CHMO also catalyzes the oxygenation of compounds containing thiols (*16*), aryl alkyl sulfides (*17*), cyclic thioethers such as thiane (*5*), or nitro groups, as well as boronic acids (*3*). The broad substrate tolerance of CHMO, coupled with the fact that many of the lactones produced are highly enantioselective, has aroused much interest for the possibility of using the enzyme to synthesize such asymmetric compounds. These chiral "synthons" can be used for the synthesis of more complex products including drugs. Several studies have shown that CHMO can be used to synthesize lactones enantioselectively

Scheme 1: Reaction of Reduced Flavin with Oxygen

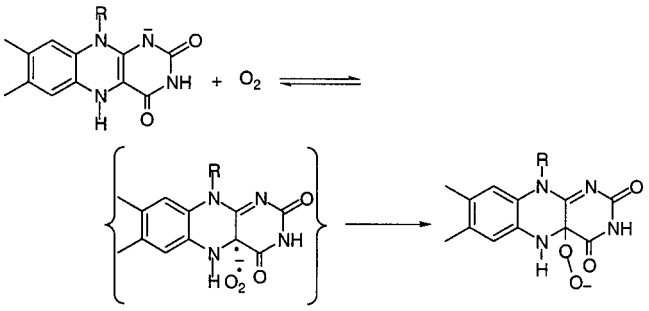

in good yield (*7*, *15*, *16*). CHMO has been expressed in baker's yeast (*Saccharomyces cerevisiae*) to provide a general reagent for asymmetric Baeyer−Villiger oxidations (*6*). In baker's yeast, the cosubstrate, NADPH, is generated biologically by fermentation of glucose, and the conversion of externally supplied cyclic ketones into the lactones occurs in vivo. Thus, no expensive cofactors need to be supplied during synthesis of products.

The kinetic mechanism of CHMO is like that for the mammalian flavin monooxygenase (FMO) from eukaryotes (*18*, *19*). As observed in previous experiments (*8*) and in the current work, the rate of reduction of CHMO by NADPH does not depend on the presence of cyclohexanone (Table 1). This contrasts with flavoprotein aromatic hydroxylases, which are reduced much faster (up to 10^5-fold) in the presence than in the absence of substrate (*20*−*22*). In this latter family of enzymes, in addition to being hydroxylated, substrates also act in a regulatory fashion, only allowing efficient reduction in their presence, and this prevents the wasteful consumption of NADPH and the production of toxic H_2O_2 in their absence. CHMO also only utilizes NADPH and oxygen rapidly in the presence of substrate, but this occurs by a different mechanism. Thus, CHMO, like FMO, becomes reduced and reacts with oxygen to form a relatively stable C4a-oxygenated flavin, which converts to oxidized flavin rapidly only when substrate is present. NADP, a product of the reduction reaction for these enzymes, remains tightly bound to the reduced forms of the enzymes and stabilizes the normally labile C4a-oxygenated flavin until substrate becomes available. Both CHMO and FMO have broad substrate tolerance (which may be part of their biological functions), so that strict control of the reduction step by substrate is not practical. However, turnover is controlled by substrate because the flavin peroxide is kinetically labile only in its presence. In addition, the expression of CHMO is induced by cyclohexanol, the precursor of cyclohexanone (*23*).

Early studies of CHMO have shown that, in the presence of NADP, a C4a flavin adduct results from the reaction of the reduced enzyme with oxygen, and this adduct leads to oxygenation of the ketone (*8*). However, this C4a intermediate had not been characterized in detail. When NADPH transfers a hydride to oxidized flavin, the immediate product is the anionic reduced flavin, which can subsequently be protonated. As shown by NMR studies, most reduced flavoproteins stabilize the anionic reduced flavin (*24*). When the reduced flavin reacts with oxygen, the first observable intermediate would be the anionic flavin C4a-peroxide as shown in Scheme 1. As shown in Figures 2−6, at low pH the C(4a) adduct of CHMO slowly becomes protonated (pK_a = 8.4), and this results in a species that is incapable of oxygenating cyclohexanone rapidly. We propose that the protonated intermediate is the flavin C4a-hydroperoxide, although protonation of an enzyme residue that led to a change in the peak position of the C4a-FAD adduct would also be consistent with our data.

The spectra of protonated model C4a-hydroperoxides are well-known and are substantially similar to those found with flavoprotein hydroxylases. However, there are no established spectra of model flavin C4a-peroxides (i.e., in the anionic state). The C4a-hydroperoxide of *N*(5)-ethyl-3-methyllumiflavin has a wavelength maximum at 366 nm in dimethylformamide (*25*) and at 370−374 nm in methanol (*26*); its spectrum (λ_{max} = 366−374 nm) is very similar to that of the flavin C4a-hydroperoxide (or peroxide—it is not yet clear whether the species is the peroxide or the hydroperoxide) found with bacterial luciferase (*27*). These values can be compared with those for the hydroperoxide species observed with *p*-hydroxybenzoate hydroxylase (382−390 nm, depending on substrate) (*28*), melilotate hydroxylase (385 nm) (*29*), phenol hydroxylase (375−390 nm, depending on substrate) (*30*, *31*), 3-methyl-2-hydroxypyridine-5-carboxylate oxygenase (385 nm) (*32*), and anthranilate hydroxylase (380−390 nm, depending on substrate) (*33*, *34*). All enzymes in the latter group catalyze hydroxylations on activated aromatic substrates. Because the mechanisms involve the flavin hydroperoxide acting as an electrophile to nucleophilic substrates, it is almost certain that the observed reactive species in the family of aromatic hydroxylases is the flavin C4a-hydroperoxide rather than the peroxide.

In the case of CHMO it is clear that the species involved in the oxygen insertion into substrate is the one with the shorter wavelength maximum (366 nm). From the nature of the reaction catalyzed, it is logical that this should be the flavin C4a-peroxide, not the hydroperoxide. The immediate covalent product from reaction of the reduced enzyme·NADP complex with oxygen is the species with a wavelength maximum of 366 nm. The chemistry between reduced flavin anion and oxygen (Scheme 1) is consistent with this covalent product being the peroxide. This species, in the absence of substrate, is in slow reversible acid/base equilibrium with a pK_a of 8.4. This is also consistent with the concept that the 383 nm absorbing species is the hydroperoxide. An alternative explanation is that the slow acid/base equilibrium is due to the state of ionization of some protein residue; this step could possibly be accompanied by a conformational change in the protein to produce a state unsuitable for catalysis. At the moment we cannot discriminate between such possibilities. However, the chemical logic of the reaction is entirely consistent with the 366 nm absorbing species being the flavin peroxide and the 384 nm absorbing species being the hydroperoxide.

In the presence of NADP, but without substrate, the C4a-hydroperoxide is surprisingly stable; thus, at pH 7.2, 4 °C, the half-life is ∼5 min (Figure 4). At pH 9.0, H_2O_2 eliminates from the C4a-flavin about 25-fold faster than at pH 7.2 (nevertheless, a slow reaction), suggesting that base catalysis is involved in the elimination of H_2O_2. Presumably, a base catalyzes the elimination by removing the N5 proton of the C(4a)-peroxide of FAD. The detailed chemistry of how NADP stabilizes the C4a oxygen flavin intermediates is not known.

Scheme 2: Possible Mechanisms of Cyclohexanone Monooxygenase-Catalyzed Oxygen Insertion into Substrate[a]

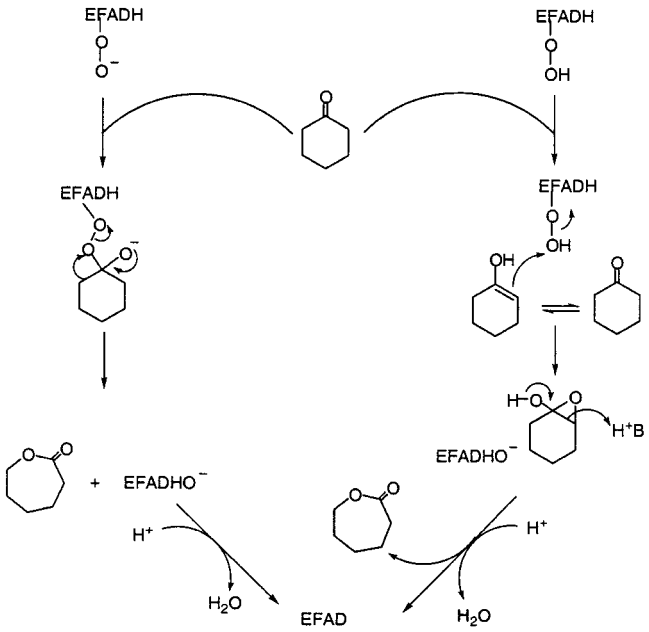

[a] From Schwab (*35*).

In Baeyer−Villiger reactions, it is thought that peroxides act as nucleophiles to attack electrophilic ketones (or aldehydes) as shown in Scheme 2 (*9*). An alternative mechanism, wherein a hydroperoxide is the electrophile that is attacked by the enol tautomer of the ketone (Scheme 2), has been shown to be unlikely with CHMO. In reactions with CHMO and [2,2,6,6-$^2H_4$]cyclohexanone, unreacted ketone and the [$^2H_4$]lactone products were shown by gas chromatography−mass spectrometry analysis to undergo no proton exchange between the deuterated substrate and the protonic solvent (*35*). Moreover, [2,2,6,6-$^2H_4$]cyclohexanone showed no kinetic isotope effect in either steady-state or rapid reaction studies (*8*). Both of these results offer strong support for the peroxide mechanism.

Here we provide clear kinetic evidence consistent with the peroxide mechanism in which the ketone substrate functions as an electrophile. Our double-mixing stopped-flow data show that the protonated intermediate (presumably the C4a-hydroperoxide) does not oxygenate the substrate. Thus, if substrate is added within milliseconds after mixing the reduced CHMO−NADP complex with oxygen (even at low pH values), oxidized FAD and product are formed rapidly. However, if the substrate is added after incubation at pH 7.2 for more than 1.5 s, no rapid formation of oxidized FAD occurs. The fraction of enzyme reacting via the fast phase to form oxidized enzyme becomes smaller as the incubation time increases up to 1.5 s, presumably because the fraction in the C4a flavin peroxide form decreases. Consistent with the notion that this is an equilibrium, the hydroperoxide can be converted back to the peroxide (∼4.7 s^{-1}), which then forms reoxidized FAD quickly, as oxygenation of substrate occurs. CHMO is designed to use the flavin C4a-peroxide at pH values that would promote formation of the hydroperoxide, and therefore its active site is constructed to prevent rapid access to protons. Nevertheless, we see that protons can exchange at rates of a few per second. Similar rates of proton exchange have been observed with a mutant form of *p*-hydroxybenzoate hydroxylase (*36*) in which the catalytically important proton network that is normally intended for rapid exchange of protons to the active site is disrupted. With this mutant form, internal protons only exchange by slow processes that are likely due to breathing modes of the protein, so that catalytic steps that are dependent on this network occur slowly. A similar breathing motion for proton exchange may also occur with CHMO.

The overall catalytic mechanism of the reaction catalyzed by cyclohexanone monooxygenase is summarized in Scheme 3, with values for rate constants collected at pH 9.0 in the presence of 0.4 M KCl at 4 °C to be described below. The oxidized enzyme reacts with NADPH via a Michaelis complex with K_d of 6.8 μM to form E−FADH$^-$·NADP$^+$ complex with a maximum rate of 22 s^{-1}. This complex reacts very rapidly with oxygen ($k \geq 5 \times 10^6$ M^{-1} s^{-1}) to form the presumed flavin C4a-peroxide anion (E−FADHOO$^-$·NADP$^+$) with a wavelength maximum of 366 nm. In the absence of cyclohexanone this species is in slow protonic equilibrium with the presumed flavin C4a-hydroperoxide (E−FADHOOH·NADP$^+$) with a wavelength maximum of 383 nm and with an observed pK_a of 8.4. The protonated species is unreactive with substrate, but the unprotonated species can undergo a rapid series of reactions with cyclohexanone ($k = 110 \pm 5$ s^{-1}) to yield an oxidized enzyme species, presumably a complex with NADP and the ϵ-caprolactone product still bound (E-FAD·P·NADP$^+$). The presumed steps consistent with a Baeyer−Villiger mechanism are shown in Scheme 3. The breakdown of the presumed Criege adduct, formation of ϵ-caprolactone, and dehydration of the flavin C4a-hydroxide must be faster than the initial reaction with cyclohexanone, because no intermediates occurring between the C4a-peroxyflavin and oxidized flavin species are distinguishable spectroscopically. The complex kinetics of the subsequent phases of the oxidative half- reaction shown in Figure 7 appear to be due to the release of the ϵ-caprolactone product ($k \sim 12$ s^{-1}) followed by the slow release of NADP via a two-step equilibrium. If the postulated release of the ϵ-caprolactone at ∼12 s^{-1} is responsible for the small spectral change associated with this phase, it must be an irreversible step, because we are unable to reverse such a change to the spectrum of oxidized enzyme by addition of ϵ-caprolactone to the oxidized enzyme, even in the presence of NADP (results not shown). The release of NADP is clearly evident from the large spectral changes observed in the 380−410 nm region in the final step of the oxidative half-reaction, which is the reverse of the observations seen with binding of NADP to the oxidized enzyme (Figure 9). The observed rate constant (3 s^{-1}) for this step in the experiment of Figures 9 and 10 is due to the approach to equilibrium between the two EFAD·NADP$^+$ species of eq 5, as shown in eq 7 (*14*).

$$k_{obs} = \frac{k_1[\text{NADP}](k_3 + k_4) + k_2k_4}{k_1[\text{NADP}] + k_2 + k_3} \qquad (7)$$

From the analysis of Figure 10 the primary rate-limiting step in the overall reaction is the conversion of EFAD*·NADP$^+$ to EFAD·NADP$^+$, occurring with a rate constant of ∼2 s^{-1}. This is consistent with catalytic turnover studies where a k_{cat} = 1.3 s^{-1} was determined under the same conditions. It is also consistent with the observation that NADP is a competitive inhibitor to NADPH in catalytic turnover (*8*) with an

Scheme 3: Proposed Mechanism of Cyclohexanone Monooxygenase

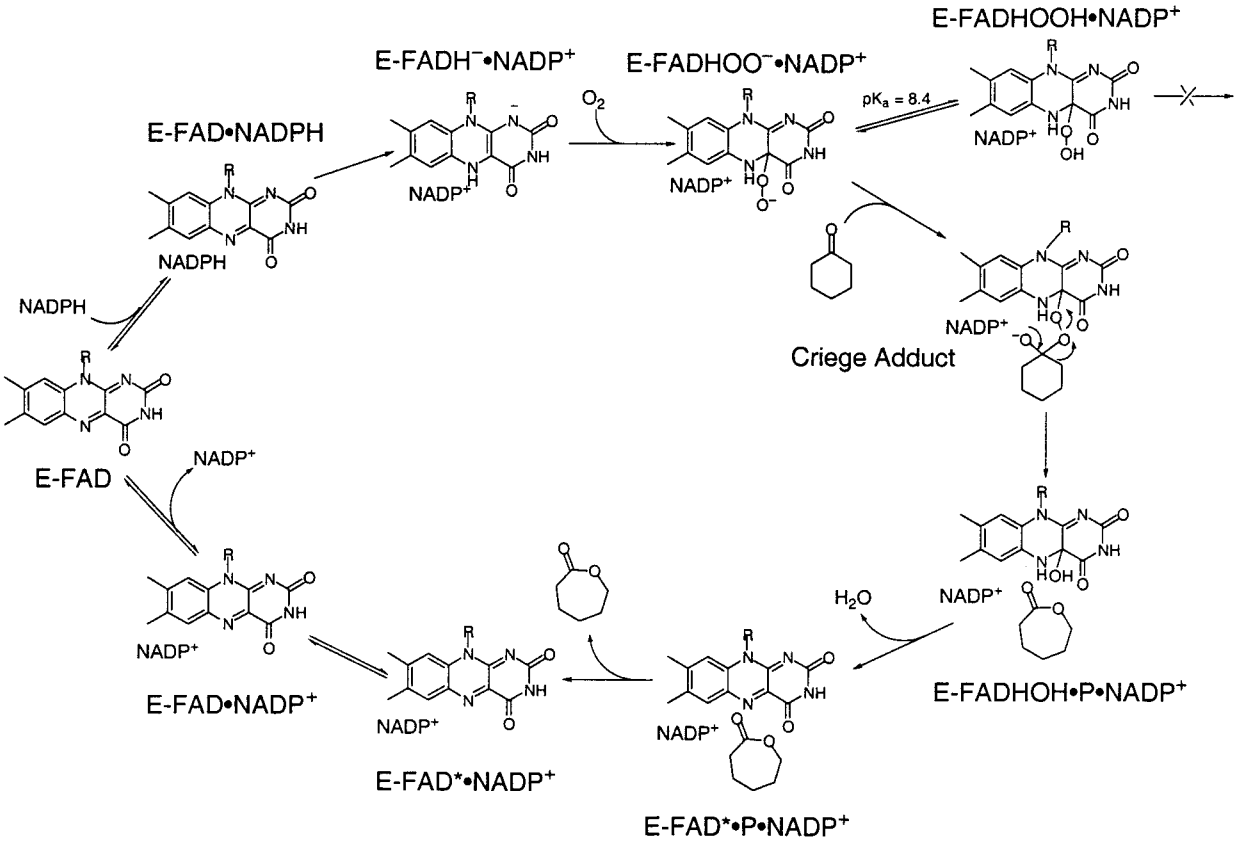

observed K_I of 38 μM at pH 9.0, 25 °C. This K_I is almost identical with the overall K_d of NADP binding to the oxidized enzyme at pH 9.0, 4 °C, measured in the present study.

An interesting prediction from this analysis is that catalytic turnover with most reactive substrates might be limited by the release of NADP from the oxidized enzyme. Although of only limited importance in the case of cyclohexanone as substrate, release of the oxygenated product might also contribute to the overall catalytic rate with other substrates. Rapid reaction studies such as those described here should be capable of differentiating among these possibilities. A similar situation holds for FMO (*37*). With that enzyme the release of NADP is also rate determining in catalysis. However, in this case NADP stabilizes the C(4a)-hydroxyflavin [as well as the C(4a)-hydroperoxyflavin before substrate is added], and when NADP dissociates, the C(4a)-hydroxyflavin intermediate quickly dehydrates to give oxidized FAD. Thus, with most substrates the k_{cat} is very nearly the same.

The spectral changes associated with binding of NADP to the oxidized enzyme are extraordinarily large and imply substantial differences in the flavin environment on binding. The two-step binding process is very clear from these spectral changes. The data indicate a rapid-equilibrium binding that is fairly weak (primary $K_d \sim 2 \times 10^{-4}$ M) followed by slow accommodation into the active site adjacent to the flavin, resulting in a tighter overall thermodynamic binding (K_d = 37 μM). Such multistep binding of ligands to proteins is probably much more common than is generally recognized. For example, it has been demonstrated recently in our laboratories with substrate binding to lactate oxidase (*38*) and to *p*-hydroxybenzoate hydroxylase (*39*) and has also been shown with another flavoprotein, D-amino acid oxidase (*40*). The phenomenon probably represents the attainment of discrete energy minima in the dynamics of protein−ligand interactions, important for establishment of the "near attack conformers" believed to be crucial in enzyme catalysis (*41*).

ACKNOWLEDGMENT

We thank Dong Xu for help in the NADP binding experiments, Dong Xu and Jonathan Pan for help in preparations of the enzyme, and Bruce Palfey for helpful discussions.

REFERENCES

1. Donoghue, N. A., Norris, D. B., and Trudgill, P. W. (1976) *Eur. J. Biochem. 63*, 175−192.
2. Norris, D. B., and Trudgill, P. W. (1976) *Eur. J. Biochem. 63*, 193−198.
3. Branchaud, B. P., and Walsh, C. T. (1985) *J. Am. Chem. Soc. 107*, 2153−2161.
4. Ahrens, M., Macheroux, P., Eberhard, A., Ghisla, S., Branchaud, B., and Hastings, J. W. (1991) *Photochem. Photobiol. 54*, 295−299.
5. Walsh, C. T., and Chen, Y.-C. (1988) *Angew. Chem., Int. Ed. Engl. 27*, 333−343.
6. Stewart, J. D., Reed, K. W., Martinez, C. A., Zhu, J., Chen, G., and Kayser, M. M. (1998) *J. Am. Chem. Soc. 120*, 3541−3548.
7. Ottolina, G., Carrea, G., Colonna, S., and Rückemann, A. (1996) *Tetrahedron: Asymmetry 7*, 1123−1136.
8. Ryerson, C. C., Ballou, D. P., and Walsh, C. (1982) *Biochemistry 21*, 2644−2655.
9. Krow, G. R. (1993) in *Organic Reactions 1993* (Paquette, L. A., Ed.) pp 251−353, John Wiley and Sons, New York.
10. Chen, Y. C., Peoples, O. P., and Walsh, C. T. (1988) *J. Bacteriol. 170*, 781−789.

11. Massey, V., and Hemmerich, P. (1978) *Biochemistry 17*, 9−16.
12. Massey, V. (1990) in *Flavins and Flavoproteins* (Curti, B., Ronchi, S., and Zanetti, G., Eds.) pp 59−66, Walter de Gruyter, Berlin.
13. Whitby, L. G. (1953) *Biochem. J. 54*, 437−442.
14. Strickland, S., Palmer, G., and Massey, V. (1975) *J. Biol. Chem. 250*, 4048−4052.
15. Roberts, S. M., and Wan, W. H. (1998) *J. Mol. Catal. B: Enzymatic 4*, 111−136.
16. Kelly, D. R., Knowles, C. J., Mahdi, J. G., Taylor, I. N., and Wright, M. A. (1996) *Tetrahedron: Asymmetry 7*, 3653−3668.
17. Light, D. R., Waxman, D. J., and Walsh, C. (1982) *Biochemistry 21*, 2490−2498.
18. Beaty, N. B., and Ballou, D. P. (1981) *J. Biol. Chem. 256*, 4611−4618.
19. Poulsen, L. L., and Zeigler, D. M. (1979) *J. Biol. Chem. 254*, 6449−6455.
20. Ballou, D. P. (1984) in *Flavins and Flavoproteins* (Bray, R. C., Engel, P. C., and Mayhew, S. G., Eds.) pp 605−618, Walter de Gruyter, Berlin.
21. Palfey, B. A., and Massey, V. (1998) in *Comprehensive Biological Catalysis* (Sinnott, M., Ed.) pp 83−154, Academic Press, New York.
22. Entsch, B., and van Berkel, W. J. H. (1995) *FASEB J. 9*, 476−483.
23. Iwaki, M., Kagamiyama, H., and Nozaki, M. (1981) *Arch. Biochem. Biophys. 210*, 210−223.
24. Müller, F. (1992) in *Chemistry and Biochemistry of Flavoenzymes* (Müller, F., Ed.) pp 557−595, CRC Press, Boca Raton, FL.
25. Nanni, E. J., Sawyer, D. T., Ball, S. S., and Bruice, T. C. (1981) *J. Am. Chem. Soc. 103*, 2797−2802.
26. Kemal, C., and Bruice, T. C. (1976) *Proc. Natl. Acad. Sci. U.S.A. 73*, 995−999.
27. Hastings, J. W., Balny, C., LePeuch, C., and Douzou, P. (1973) *Proc. Natl. Acad. Sci. U.S.A. 70*, 3468−3472.
28. Entsch, B., Ballou, D. P., and Massey, V. (1976) in *Flavins and Flavoproteins* (Singer, T. P., Ed.) pp 111−123, Elsevier, Amsterdam.
29. Schopfer, L. M., and Massey, V. (1980) *J. Biol. Chem. 255*, 5355−5363.
30. Detmer, K., Massey, V., Ballou, D. P., and Neujahr, H. Y. (1982) in *Flavins and Flavoproteins* (Massey, V., and Williams, C. H., Eds.) pp 334−338, Elsevier North-Holland, New York.
31. Detmer, K., and Massey, V. (1985) *J. Biol. Chem. 260*, 5998−6005.
32. Chaiyen, P., Brissette, P., Ballou, D. P., and Massey, V. (1997) *Biochemistry 36*, 8060−8070.
33. Powlowski, J., Ballou, D., and Massey, V. (1989) *J. Biol. Chem. 264*, 16008−16016.
34. Powlowski, J., Ballou, D. P., and Massey, V. (1990) *J. Biol. Chem. 265*, 4969−4975.
35. Schwab, J. (1981) *J. Am. Chem. Soc. 103*, 1876−1878.
36. Frederick, K. K., Ballou, D. P., and Palfey, B. A. (2001) *Biochemistry 40*, 3891−3899.
37. Jones, K. C., and Ballou, D. P. (1986) *J. Biol. Chem. 261*, 2553−2559.
38. Yorita, K., Misaki, H., Palfey, B. A., and Massey, V. (2000) *Proc. Natl. Acad. Sci. U.S.A. 97*, 2480−2485.
39. Ortiz-Maldonado, M., Ballou, D. P., and Massey, V. (1999) *Biochemistry 38*, 8124−8137.
40. Fitzpatrick, P. F., Kurtz, K. A., Denu, J. M., and Emanuele, J. F. (1997) *Bioorg. Chem. 25*, 100−109.
41. Bruice, T. C., and Benkovic, S. J. (2000) *Biochemistry 39*, 6267−6274.

BI011153H